Geomorphology 228 (2015) 213–225

Contents lists available at ScienceDirect

Geomorphology

journal homepage: www.elsevier.com/locate/geomorph

Long-term erosion rate measurements in gypsum caves of Sorbas (SE Spain) by the Micro-Erosion Meter method

Laura Sanna [a,c,*], Jo De Waele [b], José Maria Calaforra [c], Paolo Forti [b]

[a] Institute for Biometeorology, National Research Council of Italy, Traversa La Crucca 3, Regione Baldinca — 07100 Li Punti, Sassari, Italy
[b] Italian Institute of Speleology, University of Bologna, Via Zamboni 67, 40127 Bologna, Italy
[c] Water Resources and Environmental Geology Research Group, University of Almeria, Cañada de San Urbano s/n., 04120 Almeria, Spain

ARTICLE INFO

Article history:
Received 29 December 2013
Received in revised form 11 September 2014
Accepted 14 September 2014
Available online 22 September 2014

Keywords:
Micro-Erosion Meter (MEM)
Gypsum karst
Condensation–corrosion
Cueva del Agua
Sorbas, Spain

ABSTRACT

The present work deals with the results of long-term micro-erosion measurements in the most important gypsum cave of Spain, the Cueva del Agua (Sorbas, Almeria, SE Spain). Nineteen MEM stations were positioned in 1992 in a wide range of morphological and environmental settings (gypsum floors and walls, carbonate speleothems, dry conduits and vadose passages) inside and outside the cave, on gypsum and carbonate bedrocks and exposed to variable degree of humidity, different air flow and hydrodynamic conditions. Four different sets of stations have been investigated: (1) the main cave entrance (Las Viñicas spring); (2) the main river passage; (3) the abandoned Laboratory tunnel; and (4) the external gypsum surface. Data over a period of about 18 years are available. The average lowering rates vary from 0.014 to 0.016 mm yr^{-1} near the main entrance and in the Laboratory tunnel, to 0.022 mm $^{-1}$ on gypsum floors and 0.028 mm yr^{-1} on carbonate flowstones. The denudation data from the external gypsum stations are quite regular with a rate of 0.170 mm yr^{-1}. The observations allowed the collecting of important information concerning the feeding of the karst aquifer not only by infiltrating rainwater, but under present climate conditions also by water condensation of moist air flow. This contribution to the overall karst processes in the Cueva del Agua basin represents over 20% of the total chemical dissolution of the karst area and more than 50% of the speleogenetically removed gypsum in the cave system, thus representing all but a secondary role in speleogenesis. Condensation–corrosion is most active along the medium walls, being slower at the roof and almost absent close to the floor. This creates typical corrosion morphologies such as cupola, while gypsum flowers develop where evaporation dominates. This approach also shows quantitatively the morphological implications of condensation–corrosion processes in gypsum karst systems in arid zones, responsible for an average surface lowering of 0.047 mm yr^{-1}, while mechanical erosion produces a lowering of 0.123 mm yr^{-1}.

1. Introduction

The existing literature on the quantification of karst denudation by approaches of hydrochemical and flow rate measurements is relatively abundant (Corbel, 1959; Gunn, 1981; Lauritzen, 1990; Pulina and Sauro, 1993; Abu-Jaber et al., 2001; Groves and Meiman, 2005; Gabrovšek, 2009). However, there are many studies that use experimental measurements in karst terrain (Stephenson and Finlayson, 2009). Essentially, the methods most commonly used are the direct measurement by instruments generically called Micro-Erosion Meter (MEM) (High and Hanna, 1970; Smith, 1978; Trudgill et al., 1981; Stephenson, 1997; Furlani et al., 2010) or calculation of weight loss of standardized limestone (or gypsum) tablets located onsite in the study area (Trudgill, 1975; Crowther, 1983; Gams, 1986; Tarhule-Lips and Ford, 1998; Plan, 2005; Gabrovšek, 2009). The previous studies on karst denudation in gypsum areas are far less abundant than those in carbonate terrains, relative to some experiences in the gypsum karst of Spain (Calaforra, 1998), Italy (Dell'Aglio, 1993; Cucchi et al., 1996; Del Monte et al., 2000; Forti, 2005), Ukraine (Klimchouk and Aksem, 2002, 2005), New Mexico (Shaw et al., 2011) and a comparative study among some of these areas using results from rock-tablets (Klimchouk et al., 1996a). The fact that the gypsum in natural conditions is between 5 and 10 times more soluble than calcite allows the denudation in this lithology to be detected even over short time intervals. Thus the accuracy of the instrument is not a limitation as frequently occurs in carbonate terrains.

The use of the MEM experimental method enables the determination of denudation rates in very specific conditions. This is because the location of measurement points can be set in previously chosen spots with different characteristics of lithological, textural or specific environmental conditions. The short-term MEM method can suffer from incorrectly detected variations of overall denudation values in an area, which are

* Corresponding author at: Institute for Biometeorology - IBIMET-CNR, Traversa La Crucca 3, Località Baldinca, 07100 Sassari, Italy.
E-mail addresses: speleokikers@tiscali.it (L. Sanna), jo.dewaele@unibo.it (J. De Waele), jmcalaforra@ual.es (J.M. Calaforra), paolo.forti@unibo.it (P. Forti).

http://dx.doi.org/10.1016/j.geomorph.2014.09.009
0169-555X/

apparently only detectable on a large scale through mass balance calculations at the basin or aquifer scale. However, it should be noted that when measurements expand over intervals of many years, as in this case study, the obtained data can start to be significant in the validity and representativeness of the overall process of denudation (Spate et al., 1985; Stephenson et al., 2010; Trenhaile and Lakhan, 2011). The climatic implications of denudation in arid zones must also be highlighted. Normally denudation is related to rainfall in the area, and to the temporal distribution of the rain, but it also depends on the diurnal temperature variance and the role of condensation–corrosion processes (Shaw et al., 2011).

Condensation–corrosion is an important dissolutional process in speleogenesis that occurs within caves in many karst settings around the world (Dublyansky and Dublyansky, 2000), but it is scarcely studied and most of the previous works focused on condensation as a microclimatic process (Badino, 2004) and on numerical (De Freitas and Schmekal, 2003, 2006) and physical models (Dreybrodt et al., 2005; Gabrovšek et al., 2010) as a function of the vapour gradient between the cave air and cave walls and on heat flux as contribution of condensation water (Curtis, 2009). In some cases the speleogenetic importance of condensation–corrosion was highlighted, especially in hypogenic caves (e.g. Audra et al., 2007; Plan et al., 2012). Also the importance of condensation on cave morphology, especially in semi-arid regions, was highlighted (Auler and Smart, 2004) but without carrying out quantitative measurements. Large thermal variations between surface and underground environments and the presence of several entrances, allowing strong and widespread air circulation as well as highly soluble rocks cause condensation–corrosion mechanisms to become an important speleogenetic agent, as in the case of the gypsum karst of Sorbas (SE Spain) (Pulido Bosch, 1986).

In order to quantify these phenomena multidisciplinary research commenced in 1991 on the chemical corrosion of gypsum in the Mediterranean region and Cueva del Agua karst system (Sorbas district) was the first gypsum cave where various MEM monitoring stations were installed (Calaforra et al., 1993a,b; Dell'Aglio, 1993). In this paper the long-term experimental MEM data collected in this cave are presented and considered with respect to condensation–dissolution rates.

2. Study area

The gypsum karst of Sorbas is a protected natural area in the sector of Sorbas (Almeria, South-East Spain) and, thanks to its peculiar surface and underground karst morphologies, represents one of the most important evaporite karst regions in the world (Klimchouk et al., 1996b; Gutierrez et al., 2008) (Fig. 1).

In only 25 km^2, this plateau hosts more than 1000 caves, several of which develop for over a kilometre. These caves constitute a network of subterranean passages of tens of kilometres of development. Sorbas hosts the largest gypsum cave in Spain, the Cueva del Agua.

From a geological point of view this area is located in the Tabernas–Sorbas Basin, a intramontane Neogene depression in the Betic Belt where Messinian evaporite deposition occurred on silt and clay outcrops (Dronkert, 1977). The sedimentary series is represented by 16 cycles of interbedded gypsum and pelitic-marly laminated sediments with a total thickness of about 120 m and massive selenite strata up to 30 m (Roveri et al., 2009). Despite their compact appearance the gypsum layers are composed of large crystals that can be up to 2 m long. Marine sandstones, coastal plain silts and sands and continental conglomerates overlie the evaporitic series (Ruegg, 1964; Roep et al., 1979; Mather and Harvey, 1995). The structure is poorly-deformed tabular, and stratification varies from slightly inclined to sub-horizontal, with beds affected by some tilting and northward faulting playing an important role in cave development (Calaforra and Pulido-Bosch, 2003).

The climate in the Sorbas basin is semi-arid Mediterranean with an annual precipitation average of 274 mm (Maestre et al., 2013), with greater concentration occurring as high-intensity, short-duration events distributed in only 3–4 stormy days. On average, there are only 30 rainy days per year (Pulido Bosch, 2007), and despite this aridity epigenic karst morphologies are well developed because of the high gypsum solubility. The rainfall regime is characterised by minimum mean values recorded in July, whereas the maxima are registered in November. The area is mostly exposed to south-western winds that bring warm, moist air masses from Africa. The average annual temperature in the area is approximately 14.6 °C, with the minimum in January (7.3 °C) and the maximum in July (30.3 °C), so the resulting very high evapotranspiration (1190 mm yr^{-1}) (Jones and Harris, 2011) reduces the effective rain to less than 25% of the total (60 mm yr^{-1}), but probably the infiltration is even less due to the fact that the rain is concentrated in only a few storms (Calaforra et al., 1993b).

2.1. Karst of Sorbas

The particular geomorphology of the evaporite karst of Sorbas is associated with strong contrasts in lithology and structure between the gypsum itself and the surrounding sedimentary rocks. The gypsum stands out above the landscape forming a large, NE-elongated platform with sub-vertical or very steep edges looking out on dry valleys excavated on softer marls and clays. The average altitude of the top plateau is around 400 m a.s.l. (Sanna et al., 2012).

The epikarst comprises an enormous number of small dolines (more than a thousand of closed depressions have been catalogued) (Calaforra and Pulido-Bosch, 1999b), different forms of karren (mainly rinnenkarren in mesocrystalline gypsum and rundkarren in macrocrystalline ones) and wide fields of tumuli (superficial, hollow sub-circular domes) (Calaforra and Pulido-Bosch, 1999a). Most of these relief features are related to the extensive subterranean karst network present beneath the arid gypsiferous desert of Sorbas. Dolines rapidly collect runoff at the surface and allow rainwater infiltration, reaching the spring in only a few days after rainfall. Currently water seepage between the gypsum crystals and along the exfoliation planes is very scarce, affecting only the first centimetres of rock and just the interbedded marls have some storage capability. Underground cave development follows the orientation of the surface network and derives from the gradual dissolution and erosion of the evaporite rock along the planes of weakness in contact with the marly, less permeable base. Characteristic cave morphologies are triangular interbedded passages (Calaforra, 1986). Once the infiltrated water reaches the caves, it tends to evaporate and leaves mineral salts in the form of gypsum and carbonate speleothems (stalactites, stalagmites and many other forms). Thus the speleogenetic evolution of the caves of Sorbas is intimately linked to the hydrogeological history of the area. After an initial phreatic phase, during which water flowed in gypsum protoconduits, the progressive lowering of the base level brought these voids to shift into vadose conditions initiating the mechanical erosion of the marls and the enlargement of the cave passages. Once the less permeable basement was reached, the discharge fluctuations partially filled the cave passages with the overlying clastic materials eroded from the surface. Precipitation of the carbonate and gypsum speleothems occurred during these late stages (Calaforra and Pulido-Bosch, 2003). The edge of the gypsiferous plateau is characterised by the presence of a number of springs, mainly connected to one of the most important underground rivers which discharges water from this karstic area and is currently independent from allogenic catchment contributions, indicating the presence of other alternative water sources different from rainfall. Freshwater outflows occur through gypsum fissures and at the contact between gypsum and marls, with large variations in flow as an immediate response to heavy rainfall. Most of the rainwater infiltrated in this basin eventually emerges at Los Molinos spring, the largest in the district, with a flow of around 70 L s^{-1} — a considerable amount for this semi-arid area (Pulido Bosch and Calaforra, 1993). A modest outlet directly related to a large gypsum cave is Las Viñicas, which drains the Cueva del Agua.

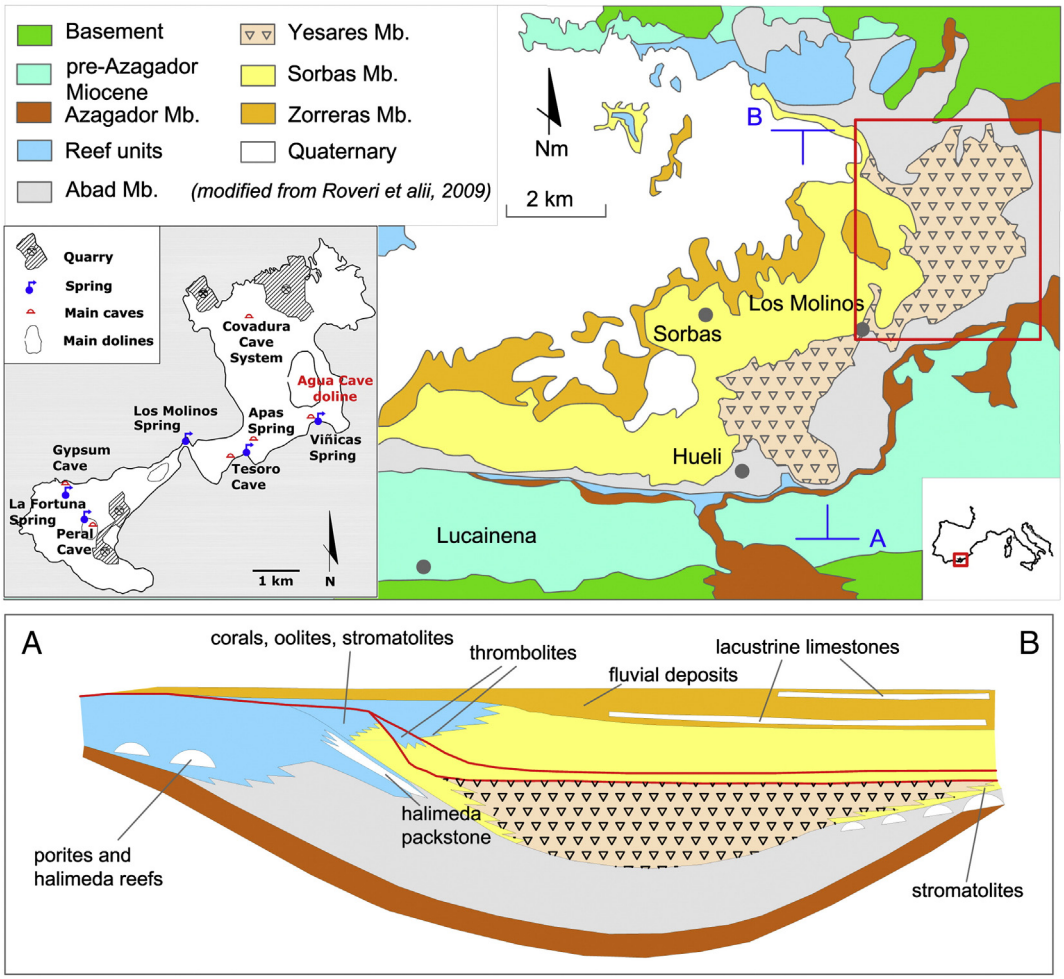

Fig. 1. Geological sketch map of the Sorbas Basin and profile at section A–B, the same geometry across the study area (red square). Inset shows some of the important karst sites. The bold line represents the macrodoline of Cueva del Agua (modified from Sanna et al., 2012). (For interpretation of the references to colour in this figure legend, the reader is referred to the web version of this article.)

2.2. Cueva del Agua

Cueva del Agua or Marchalico karst system drains a wide closed depression 1.5 km^2 in size, located in the north-eastern part of the Sorbas plateau, representing one of the most characteristic endorheic basins of the area (Fig. 2). This depression hosts more than one hundred dolines per km^2, the highest density of Spain. The Cueva del Agua, with its labyrinth of underground passages, has more than 33 explored entrances (but it is reasonable to suppose the presence of hundreds of them) and extends over more than 8.9 km (currently the most extensive in Andalusia), reaching 50 m depth (Espeleo Club Almeria, personal communication).

Its sub-horizontal conduits develop in a NW-SE direction, a few metres below the surface, and are accessible through several small vertical shafts that represent upper entrances. An underground stream feeds the Las Viñicas spring (356 m a.s.l.) with a low water discharge of less than 1 L s^{-1} (around 0.8 L s^{-1}) and a peak discharge of about 150 L s^{-1}, occurring suddenly after heavy rainfall, flooding the lower conduits completely during a few hours and with a steep depletion curve just after rainfall ends (Calaforra, 1986). An ephemeral outlet is Tropplein cave (383 m a.s.l.), which drains a usually inactive passage that develops parallel to the main underground river and collects the rainfall through some small dolines. The geometric settlement of Sorbas massif does not allow any recharge of this cave system from adjacent basins.

Air circulation inside the cave is very complex and driven by thermal disequilibrium between outside and inside air and water temperatures (annual mean temperature in the main gallery ranges between 15 and 17 °C, whereas average water temperature is 14.5 °C) (Calaforra et al., 1993b). Las Viñicas spring (the main cave entrance) behaves as the lower entrance during most of the year, with air flow directed towards the outside, while the numerous small vertical shafts represent upper entrances that inhale moist air. The cave atmosphere is characterised by water-saturated air and only near the cave openings the relative humidity decreases up to values of 40% (Fig. 3).

Close to the main entrance (Las Viñicas spring) and also in the intermediate sectors of the cave, conduits are of phreatic origin, with rounded cross-sections, later filled by clastic sediments and covered by carbonate flowstones, deposited once the water level fell. Further upstream from the spring, the passages and shafts are generated in vadose conditions. These kinds of galleries correspond to different patterns of karst system development and some of them are currently completely abandoned by the underground river. Cave morphology is also characterised by typical condensation–corrosion features such as bell-shaped domes and boxworks. In the vadose galleries most speleothems are made of gypsum, while within the active sector calcite speleothems are found more often (Calaforra et al., 2008).

3. Methods

Direct measurement of denudation using a Micro-Erosion Meter (MEM) was initially developed by Hanna (1966) in cave conduits in

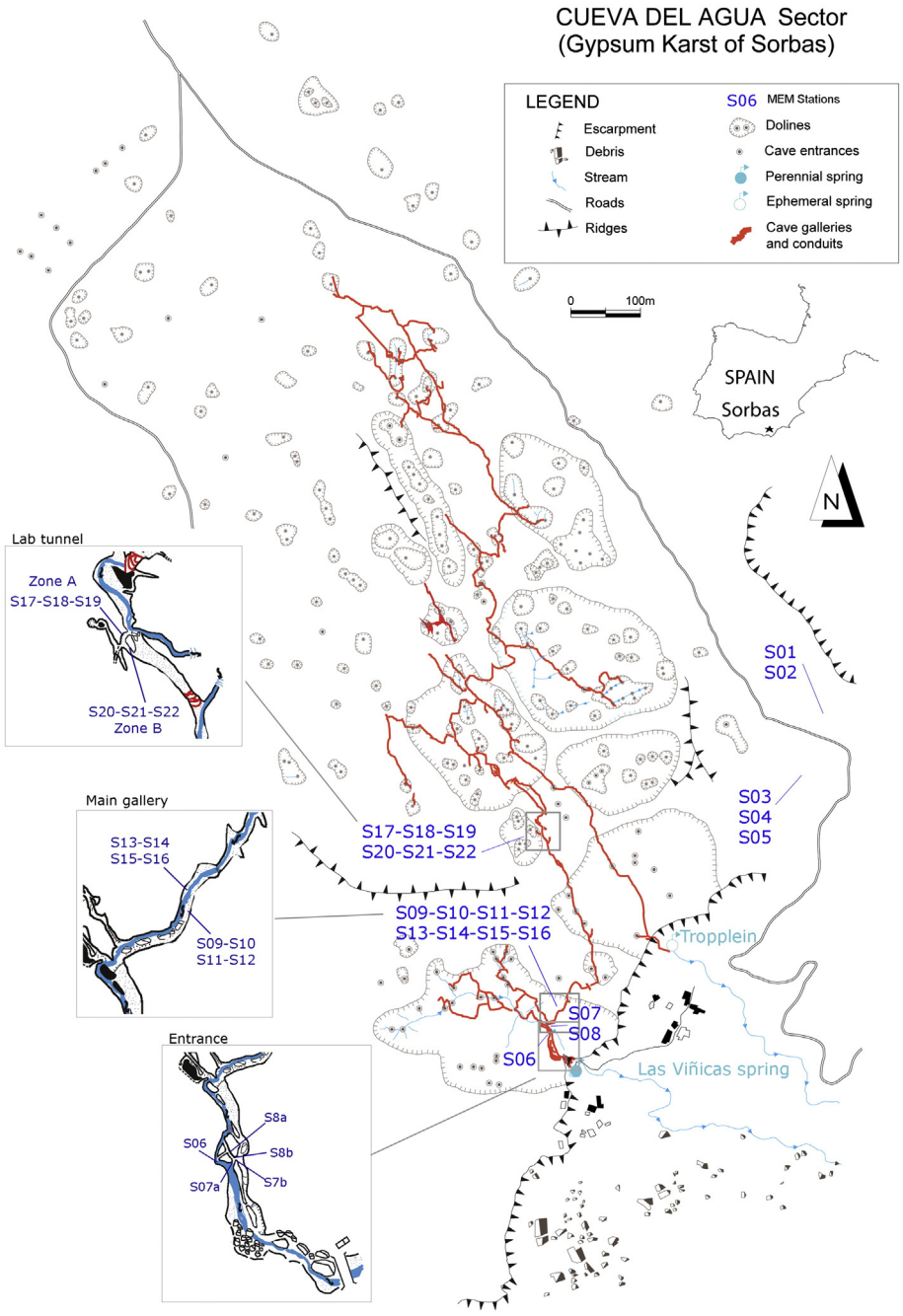

Fig. 2. Geomorphological sketch map of the Cueva del Agua area (see Fig. 1 for location). The positions of the MEM stations are indicated by blue numbers and detailed maps along the cave passages are shown in the insets (modified from Dell'Aglio, 1993; cave survey from Espeleo Club Almeria). (For interpretation of the references to colour in this figure legend, the reader is referred to the web version of this article.)

England and by Dahl (1967) on granite in Norway, and later extended and improved by High and Hanna (1970) and Trudgill (1970) in England and by Ford (1971) in Canada. Then, some improvements to the instrument were made by Trudgill et al. (1981) and finally Stephenson (1997) and Stephenson and Finlayson (2009).

The MEM method basically consists of a probe connected to a millesimal-resolution micrometer gauge (with graduations of 0.005 mm) on a tripod structure. The instrument directly touches on three stainless steel nails set into the rock surface, two with semi-spherical heads and a flat one (Fig. 4A). One of the three legs of the micrometer is semi-spherical and the other two are of pinacoidal shape. This disposition leads to six kinematic vinculums, three that restrict translational movement and the other three preventing rotation. This configuration, called Kelvin Clamp Principle, guarantees that the point where measurement is performed, the central part of the triangle formed by the three nails, is always exactly the same (Stephenson et al., 2010). In practice, because it is easy to combine several MEM measurement triangles, each measurement point can be constructed in order to obtain several stations depending on the number of the installed nails. The micrometer gauge is firmly fixed to the leg supports, thus allowing highly accurate analyses of rock lowering rates (Spate et al., 1985). The instrument is checked periodically by laboratory measurements on a calibration slab of rock at a given temperature (Furlani et al., 2009) as well as in field at the MEM stations, on a stainless steel support. This value is subtracted at each reading to calculate the net lowering. Readings below 0.010 mm must be considered with caution (Stephenson and Finlayson, 2009). Downwearing measurements were taken by two repeated readings at the same station, to reduce the source of error

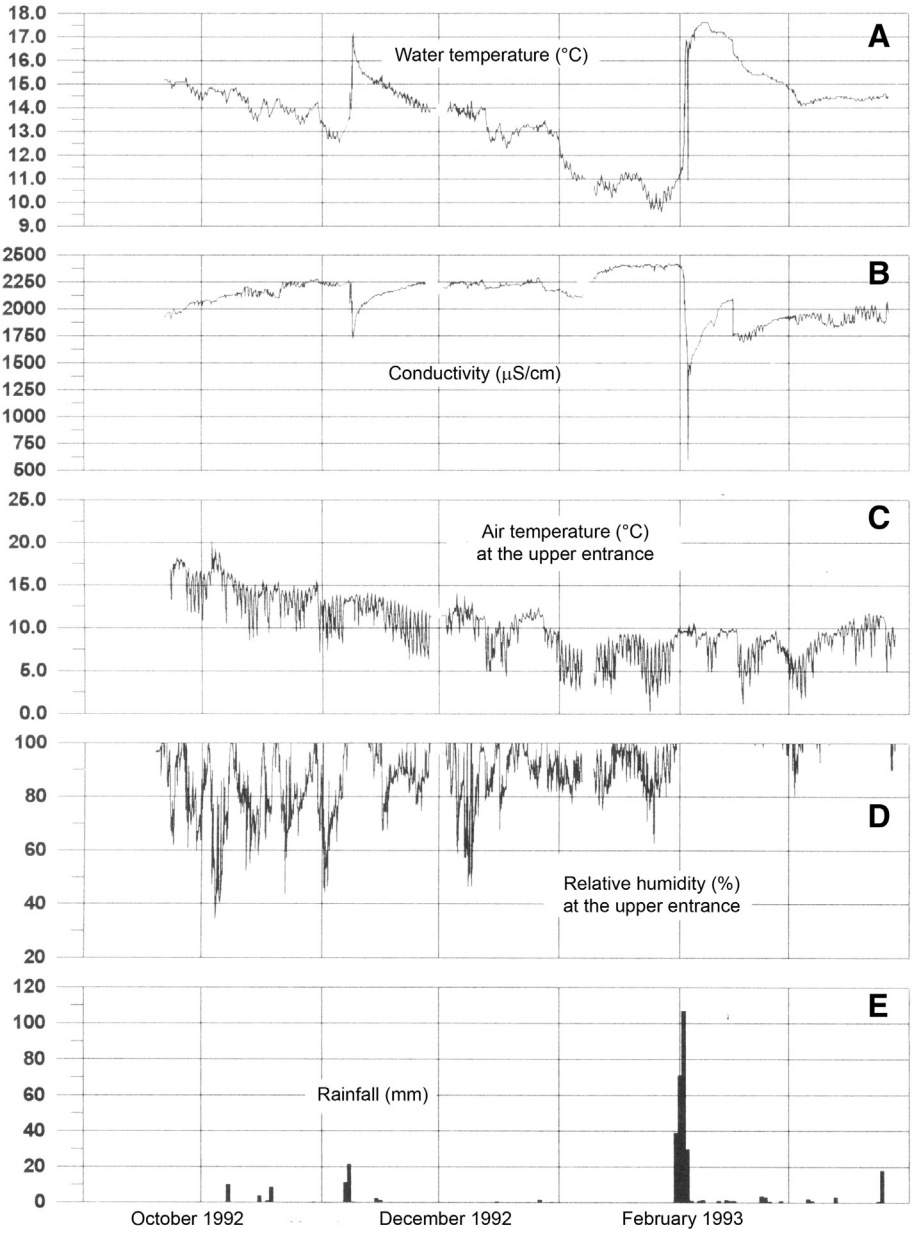

Fig. 3. Relationship between cave micrometeorological data of Cueva del Agua and pluviometry during 1992–1993. A. Water temperature of the underground stream; B. Conductivity of the stream water; C. Air temperature close to one of the upper entrances; D. Relative humidity variation close to the cave openings; this value is stable at 100% in the interior of the cave (Laboratory tunnel and along the main cave passages); E. Rainfall pattern at the Sorbas meteostation (modified from Calaforra, 1998).

due to the erosion performed by the probe tip on the soft gypsum surface and thus producing an apparent lowering. Trenhaile and Lakhan (2011) report that about 10 measurements at each point would normally provide reasonable estimates of surface elevation changes. The values reported for gypsum are more reliable than those for other kinds of less soluble rocks because their lowering rates are much greater, thus reducing the significance of errors. Also long periods of observation drastically reduce the uncertainties (Spate et al., 1985).

Nineteen MEM stations (indicated with progressive numbers, see Fig. 2) were positioned in a wide range of morphological and environmental settings inside the cave, on two bedrock types (gypsum and carbonate) and with variable degree of humidity (from 40% to 100%), and different hydrodynamics and air flow conditions: (i) on gypsum on the floor of the passages, (ii) on carbonate speleothems, and (iii) on walls and roofs where water comes in contact with the rock exclusively by condensation processes. In particular, three different sets of stations have been investigated: (1) the main cave entrance (Las Viñicas spring), where the influence of rapid temperature and humidity fluctuations at the surface is more intense (Fig. 3); (2) the main passage, in which the underground stream can flow on gypsum and on carbonate floor; (3) the Laboratory tunnel, an abandoned passage without present day water flow. Another 5 additional measurements were collected on MEM stations installed on the external gypsum surface. All sites are listed in Table 1.

In the cave entrance, not far from the spring, five MEM stations are located: one on a black horizontal calcite flowstone located in laminar flow conditions in the active cave passage (station S06, Fig. 4C) and four at half height on vertical gypsum walls in a fossil branch: two of them directly exposed to moist air coming from the internal part of the cave (stations S07a and S08a, see Fig. 4B), thus in the wet part of the cave wall, and the other two are placed on the conduit wall oriented toward the main entrance, thus in drier conditions (stations S07b and S08b, respectively).

Fig. 4. MEM stations: A. Micro-Erosion Meter; B. Measurement station at S08a on the wall; C. Floor station number S06 on carbonate flowstone close to the main entrance; D. Stations S13 to S16 on the carbonate floor along the main passage and scheme of the arrangement of nails (the finger indicates the lower vertice of the triangle on the left of measurement point); E. Medium station S21 on the wall in the Laboratory tunnel; F. Stations S09 to S12 on the gypsum floor at the measurement point in the active branch. In the background, on the other side of the stream the arrow indicates the multistation S13-S16 on carbonate flowstone (Photos Laura Sanna).

The stations in the main passage are within some hundred metres from the main entrance in the same stream level (a few centimetres above the water level, thus sporadically flooded) but displaced in two different sub-horizontal sites, one in front of the other: stations S09, S10, S11 and S12 (Fig. 4F) have been positioned on gypsum bedrock, while stations S13, S14, S15 and S16 have been installed on carbonate crusts (Fig. 4D). All sites are arranged with 6 nails forming four triangles, thus providing four measurements (see Fig. 4D).

Table 1
Main features of the MEM stations in gypsum karst of Sorbas.

MEM station	Location	Lithology	Description
S01	Surface	Selenite macrocrystalline gypsum	Flat area, sub-horizontal
S02	Surface	Selenite macrocrystalline gypsum	Flat area, sub-horizontal
S03	Surface	Selenite macrocrystalline gypsum	On a tumulo, with evident gypsum exfoliation karren
S04	Surface	Selenite macrocrystalline gypsum	Small ephemeral stream channel
S05	Surface	Selenite macrocrystalline gypsum	Area with small morphological step
S06	Cave entrance	Carbonate speleothem	Horizontal, on black carbonate flowstone. A laminar water flow is present almost during all the year, while turbulent flux occurs during floods.
S07a-S08a	Cave entrance	Selenite macrocrystalline gypsum	On a vertical gypsum wall, exposed to moisted air circulation
S07b-S08b	Cave entrance	Selenite macrocrystalline gypsum	On a vertical gypsum wall, in dried condition
S09-S10-S11-S12	Main cave gallery	Selenite macrocrystalline gypsum	Sub-horizontal gypsum floor
S13-S14-S15-S16	Main cave gallery	Carbonate speleothem	Sub-horizontal black carbonate flowstone
S17-S18-S19	Lab tunnel – zone A	Selenite macrocrystalline gypsum	Vertical gypsum wall, at the top, middle and bottom, respectively
S20-S21-S22	Lab tunnel – zone B	Selenite macrocrystalline gypsum	Vertical gypsum wall, at the top, middle and bottom, respectively

All stations of the Laboratory tunnel are on vertical gypsum walls, but separated into two distinct zones and arranged at different heights: at the top, in the middle and at the bottom of zone A, upstream of the fossil gallery (stations S17, S18 and S19), and zone B, in the central part of the Laboratory tunnel (stations S20, S21 and S22).

The first 5 measuring sites are located at the surface (stations S01, S02, S03, S04 and S05), in an area of exposed bedrock at the eastern margin of the closed depression of the Cueva del Agua doline (Fig. 2).

4. Results

The micro-erosion measurements carried out inside the cave started from June 1992, when the reference elevations were recorded at the beginning of the study, and have been taken four times during the 18 years of monitoring, one after a short period (October 1992), the second in January 1994, the third thirteen years later (April 2007) and the last in July 2010. The first two readings (the reference elevations and the measurements in October 1992) were performed with a MEM produced at Trieste ("Trieste 1" instrument). For the third record "Bolonia 1" instrument calibrated in Bologna was used. The last readings have been carried out with a new instrument produced at University of Almeria, but equivalent to the "Bolonia 1" instrument. The measurements are comparable since the instruments have been calibrated among each other. The results of the net elevations measured at each station are presented in Table 2. This table contains the period of surveying and the mean annual lowering rate calculated for each station.

The maximum duration of the measurements was 6611 days, concerning almost all stations, except for two of them in which monitoring started four months later. Some stations positioned close to the water of the cave stream have been partially flooded, so the reading was sometimes impossible. The average lowering rates vary from 0.014 to 0.016 mm yr^{-1} near the main entrance and in the Laboratory tunnel, 0.022 mm yr^{-1} on gypsum floors, and 0.028 mm yr^{-1} on carbonate flowstones. These values show a similar order of magnitude as those measured in carbonate karst areas (Häuselmann, 2008; Furlani et al., 2009; Gabrovšek, 2009).

As regards the vertical gypsum walls, a spatial gradient in the same site seems to occur: in the entrance part of the cave, stations placed on the wall oriented toward the lower entrance and not exposed to the moist cave air (stations S07b and S08b) show lower rates, as well as those close to the floor (bottom) of the Laboratory tunnel (stations S19 and S22) (Fig. 5e–f).

In the case of stations S07a and S08a, the control points were placed on vertical walls trying to put the nails in the areas where condensation appears to be greatest (related to sub-horizontal air currents, located at a medium height on the wall).

For the stations in the Laboratory tunnel (stations S17 to S22), the highest measurement points were placed in condensation cupola.

In the medium walls (Fig. 5c–d) rock surface downwearing rates were higher than top and bottom stations.

Of the four bottom (lower) stations, three report oscillations between negative (downwearing) and positive (swelling) values (S08b, S19, S22), while one shows only a very small lowering (S07b) (Fig. 5e–f).

In general, values of surface elevation changes are higher on gypsum surfaces with respect to carbonate flowstones. However, surprisingly, the lowering rates on some carbonate surfaces are greater than those registered on gypsum (e.g., stations S14 and S15, see Fig. 6a–b). The values recorded at station S16 (spatially in close proximity to the stream) has been removed from the graph due to the high variability of the readings. In some cases, the downwearing rates are not consistent between the various measurement points and seem controlled by

Table 2
MEM station measurements: monitoring spans over 18 years, with different time periods between readings. All lowering values are expressed in mm (n.d.: not-determined). The measurements at 126 days were made with the "Trieste 1" instrument, the one at 579 - days with the "Bolonia 1" instrument, while the remainder with the "Almeria" MEM.

	Elapsed time (days)				
Station ID	126	579	5408	6611	mm/a
Surface (exterior)					
S01	−0.03	−0.36	−3.36	−4.14	−0.229
S02	−0.06	−0.44	−2.43	−2.95	−0.163
S03	−0.06	−0.59	−3.10	−3.22	−0.178
S04	−0.02	−0.33	−1.46	−2.03	−0.112
S05	−0.04	−0.37	−1.59	n.d.	n.d.
Mean					*−0.170*
Cave (entrance, gypsum wall)					
S07a		−0.26	−0.27	−0.40	−0.022
S07b		−0.04	−0.07	−0.10	−0.006
S08a		−0.13	−0.40	−0.41	−0.023
S08b	0.03	0.07	0.02	−0.08	−0.005
Mean					*−0.014*
Cave (main gallery, gypsum floor)					
S09	−0.04	−0.39	−1.22	−0.74	−0.041
S10	−0.02	−0.18	−0.36	−0.50	−0.028
S11	0.01	−0.07	−0.16	−0.30	−0.017
S12	−0.06	0.01	−0.15	−0.01	−0.001
Mean					*−0.022*
Cave (carbonate flowstone)					
S06	0.00	−0.11	−0.18	−0.15	−0.008
S13	−0.01	−0.03	0.01	−0.20	−0.011
S14	−0.03	−0.27	−0.32	−0.41	−0.023
S15	0.03	0.03	0.03	−0.44	−0.025
S16	−0.03	−0.07	−3.11	−1.28	−0.071
Mean					*−0.028*
Cave (Lab tunnel, gypsum wall)					
S17 high	−0.00	0.00	−0.04	−0.14	−0.008
S18 med	−0.01	−0.01	−0.13	−0.54	−0.038
S19 bott	−0.03	0.06	−0.05	0.05	0.003
S20 high	−0.03	−0.06	−0.16	−0.19	−0.011
S21 med	0.00	−0.23	−0.36	−0.65	−0.036
S22 bott	0.00	−0.39	−0.35	−0.07	−0.004
Mean					*−0.016*

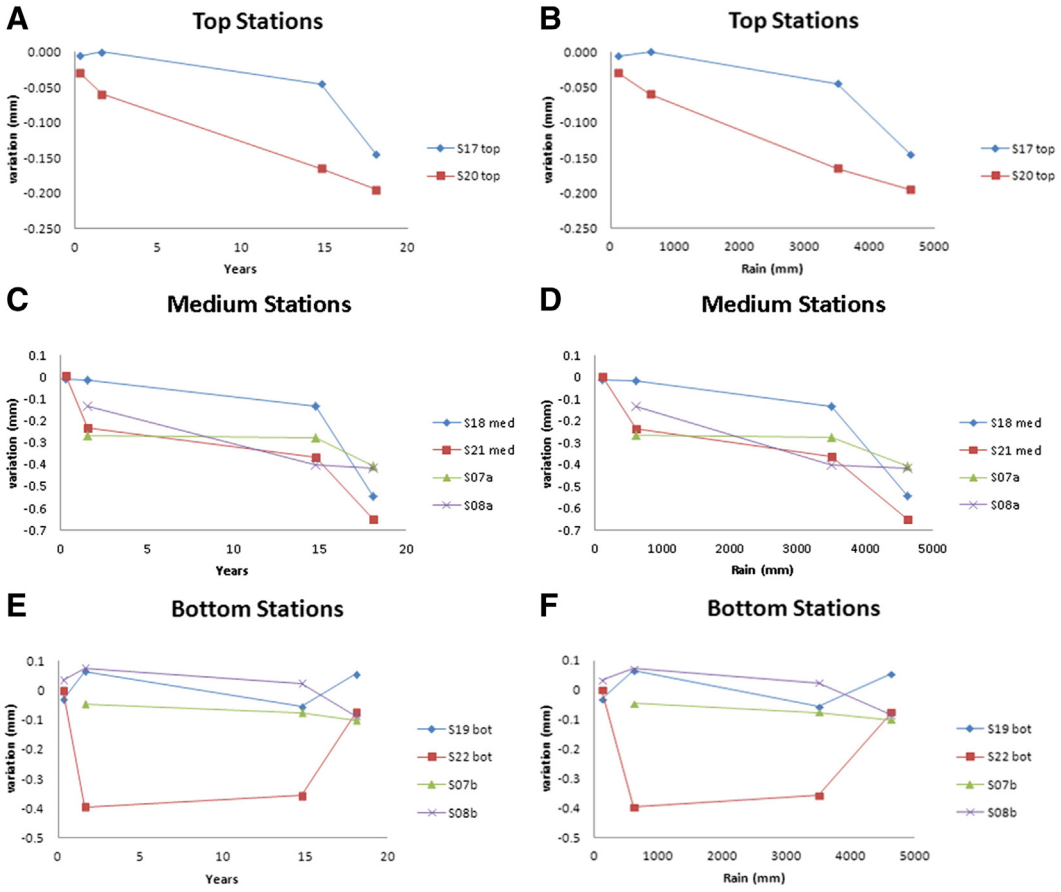

Fig. 5. Lowering values with respect to time (left) and rainfall (right) for top, medium, and bottom stations on the wall. Due to their little variation, stations S07b and S08b have been represented together with the bottom stations in the Laboratory tunnel.

factors that vary from point to point (e.g., transported clastic materials, flow intensity, etc.). In two cases (last measurement of station S06 and the penultimate measurement of station S13, see Fig. 6a–b) an obvious increase was encountered.

Mean lowering rates on gypsum are generally a little bit higher on the sub-horizontal surfaces than on cave walls, except for some of the half-height — medium — wall stations.

The denudation data from the external gypsum stations are quite regular, with a rate of 0.170 mm yr^{-1} (Fig. 6e), almost an order of magnitude greater than the mean obtained from all cave stations (0.021 mm yr^{-1}) and close to 0.3 mm yr^{-1} calculated based on mass loss of gypsum tablets in the Gypsum Plain (New Mexico) (Shaw et al., 2011). There is a good linear trend between surface denudation and rainfall (Fig. 6f). The slightly lower value of station S03 measured in the last 3 years clearly depends on factors related to the measurement point (S03 is on a tumuli feature, so gypsum swelling might have occurred). The slope of the various lines is obviously dependent on local conditions such as the steepness of the measuring point, the orientation of gypsum crystals, water flow, and so on.

5. Discussion

5.1. Condensation–corrosion as a global speleogenetic agent

Just a very marginal role was attributed to the process of condensation–corrosion in speleogenesis in the past. Its real importance in the formation of caves has been highlighted only in the last decades through the development of several investigations in carbonate environments (Cigna and Forti, 1986), and in gypsum (Pulido Bosch, 1986). In the case of gypsum the much more soluble rock evidences the prominent role of condensation–corrosion in speleogenesis, especially in arid environments.

The condensation–corrosion, and also the related rock lowering rate, has an influence on karst morphology, because the evaporation–condensation processes are able to continuously wet the cave walls with undersaturated water (Badino, 2010). The characteristic features originated from this process, such as the protruding of less soluble lithology from the rock matrix (boxwork), are very different from those due to running waters, especially in gypsum where condensation–corrosion types are easier to find. In the case of gypsum karst the dissolution by condensation inside a cave tunnel is obviously balanced by the formation of speleothems through evaporation in nearby places or at a certain distance where these water films become saturated. Although both corrosion and deposition phenomena can be localised inside several cave systems, the presence of widespread and well-developed condensation–corrosion forms is not sufficient to state that this process contributes significantly to the overall speleogenesis of a cave. It is also necessary that the cave microclimate shows large thermal variations and the karst system is characterised by several entrances, thus allowing strong and widespread air flow inside the cave passages in order to promote evaporation of the solution.

As reported in preliminary short-term studies (Calaforra et al., 1993a,b; Dell'Aglio, 1993), Cueva del Agua cave system is an ideal place where the climatic effect is clearly represented due to the high number of upper entrances that connect the cave and external atmosphere, its constant strong air circulation and its well-defined catchment area hydraulically isolated from other neighbouring catchment areas. In fact the high thermal non-equilibrium condition between

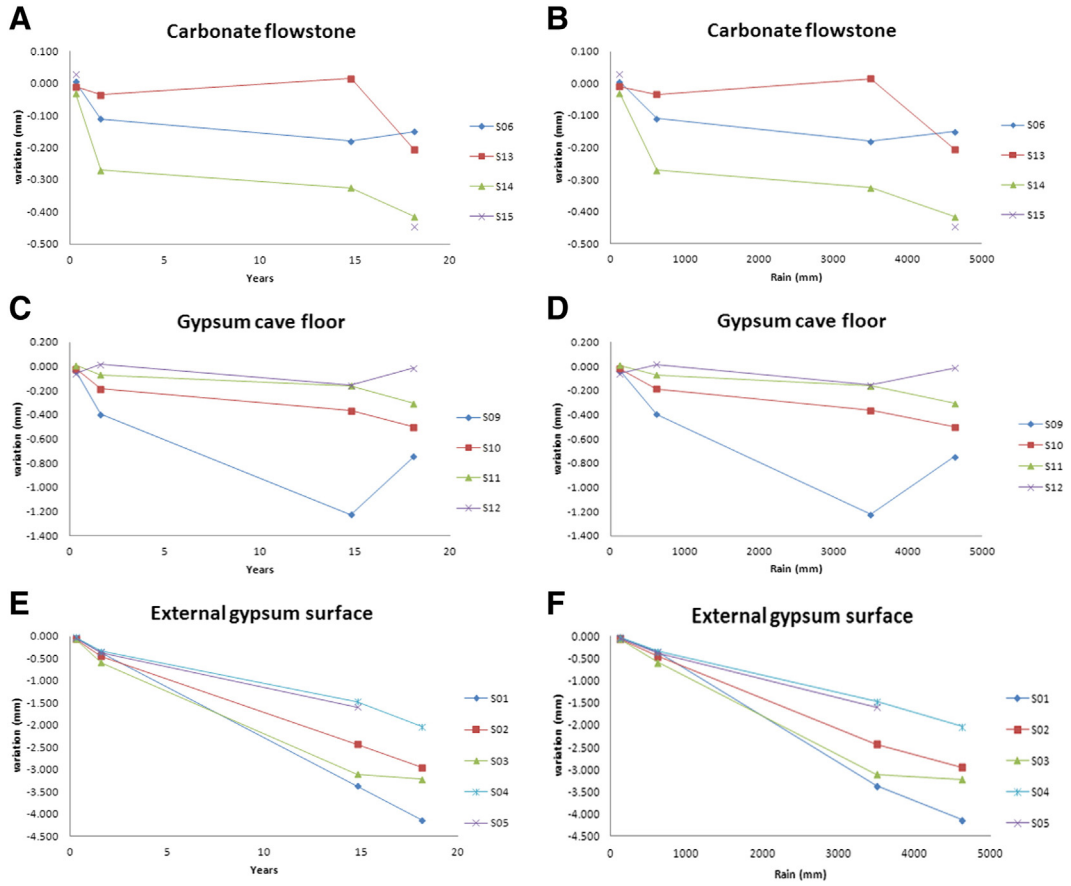

Fig. 6. Lowering values of carbonate and gypsum floor in the cave and on the external gypsum bedrock, with respect to time (left) and cumulative rainfall (right).

cave stream water (average 14.5 °C) and diurnal external air entering into the karst system (mean 19 °C) guarantees that the arid climate of the area greatly affects the meteorological behaviour of this cave.

Considering a relative humidity near 70% and a temperature of 25 °C (normal value for sunny days through the year) the external air would have more water vapour than cave air (16.2 g m^{-3} instead of 12.7 g m^{-3}) (Badino, 1995). Typical experimental values of air velocity measured in the 33 known entrances of Cueva del Agua cave system are higher than 1 m s^{-1}. Hypothesizing four hundred 0.5 m^2-sized cave inlets, the mean volume of air entering into the cave might be estimated as about 200 m^3 s^{-1}. This air flow would produce around 0.7 L s^{-1} of condensation water and justifies the water volume discharged by the cave also during the long dry periods, a base flow fed only by condensation water (<1 L s^{-1}). This analytical approach was confirmed by several micro-dye tracer experiments (Calaforra et al., 1993b) and by an ongoing experiment of direct collection of condensation water on artificial support (Calaforra et al., 2011) that gave an idea of the amount of water which may condense in a single place on each square metre (0.006 L s^{-1}). Using the cumulative rain during the 18-year long monitoring period (4630 mm), the effective infiltrating rain (25% of the total) on the 1.5 10^6 m^2-wide Cueva del Agua catchment area is about 1,735,000 m^3. On the basis of the previous estimation of cave air flow (200 m^3 s^{-1} with a condensation rate of 0.7 L s^{-1}) the condensation water for the same period (6611 days) is around 400,000 m^3, a contribution of the condensation–corrosion to the total chemical dissolution of the area of around 20%.

Moreover chemical analyses of water and experimental data of weight-loss gypsum tablets (Calaforra et al., 1993a,b; Dell'Aglio, 1993) indicate that the waters in the Cueva del Agua underground stream are always undersaturated with respect to gypsum (2.13 g L^{-1} compared to the 2.4 g L^{-1} of maximum concentration in pure water at 15 °C) (Klimchouk, 2000).

Despite the lack of long time-series monitoring, the available hydrodynamic data at the Las Viñicas spring (Calaforra, 1998) demonstrated that during 70 days per year the average discharge is around 15 L s^{-1}, giving an estimated volume of 91,000 m^3 of water discharge. After high flows water takes about a few hours to a maximum of ten days in restoring the previous low water discharge values of conductivity (from 1.7 mS/cm during floods in December 1992 to 2.4 mS/cm in low water discharge, Fig. 3B), temperature, and saturation degree. Considering an average rate of 60 mm yr^{-1} for the effective infiltration over the Cueva del Agua catchment area, the mean annual recharge of the Las Viñicas spring has been calculated as about 90,000 m^3 (practically equal to the high flow discharge), demonstrating the absence of storage capacity in the gypsum karst aquifer (those of the rare thin marl interbeds is insufficient) (Calaforra, 1986). The total discharge at the spring would be about 111,000 m^3, 20,000 m^3 of which coming from the base flow (18%).

On the basis of hydrochemical data on the Cueva del Agua stream, Pulido Bosch and Calaforra (1993) observed that the different water saturation between rain and flood waters is due to the fact that rainy water, very aggressive at first, loses much of its potential dissolution capability becoming relatively saturated with respect to gypsum within the first few metres of its subterraneous path. Only during periods of heavy rainfall, when infiltration is tremendously rapid, low water saturation is maintained inside the caves. For this reason strong karstification in a semiarid climate, such as Sorbas, can be considered as a sporadic phenomenon in the vadose zone, where cave enlargement is improved only during periods of torrential deluge whereas for most of the year only very slow processes are active.

Taking into account the gypsum water content at the spring during flood events (2.13 g L^{-1}) it is possible to estimate the chemically-removed gypsum by the rain over the 18 years of monitoring as about 3690 t (204 t yr^{-1}) while, using the average gypsum content of the spring water during the dry periods (a standard maximum value of 2.5 g L^{-1} at 20 °C) rough quantitative data on the corrosion by air condensation reaches an amount of 1000 t (55 t yr^{-1}), corresponding to 21% of the total. Considering that only some 20% of the effective infiltrated rain (percentage of rainstorms) is able to produce chemical dissolution, the amount of gypsum dissolved from the rainwater flowing into the cave (calculated over the same 18 years) is 738 t (40 t yr^{-1}) for a total underground removed quantity of gypsum of about 1735 t (100 t yr^{-1}), confirming the 1000 t of dissolved gypsum by condensation water.

The contribution of the condensation–corrosion to the overall karst processes (55 t yr^{-1}) in the Cueva del Agua basin represents over 20% of the total chemical dissolution of the karst area but more than 50% of the speleogenetically removed gypsum in the cave system. These processes, at least in the present climate, are of considerable importance in speleogenesis of gypsum caves.

5.2. Measurement of climate-induced processes

Along the main gallery of Cueva del Agua the MEM measurements show dissolution processes active on the walls and ceiling, related to condensation waters.

The maximum observed value for such dissolution was 0.41 mm in 3 years (mean 0.038 mm yr^{-1} over the 18-year period) at station S18, at half height on the wall in the Laboratory tunnel. An almost identical mean annual value (0.036 mm yr^{-1}) was recorded at station S21, located in a similar position, while the average measurement near the roof and close to the floor gave 0.0085 mm yr^{-1} and 0.0035 mm yr^{-1}, respectively. Thus, in the Laboratory tunnel the two groups of locations show the following behaviour: a slow dissolution near the roof (stations S17 and S20), a more evident downwearing rate in the middle (stations S18 and S21) and very low dissolution towards the floor (stations S19 and S22). The different trends shown at the two roof stations (S17 and S20) depend on the relative positions of each measurement point. In fact station S17 was placed almost at the top of a cupola while station S20 was located slightly lower. Therefore it is evident that the latter has more often been subject to film flow conditions (Fig. 5a–b).

In the whole of cave passages, the medium walls rock surface downwearing rates (Fig. 5c–d) were higher than the top and bottom stations, most probably due to a more regular presence of condensation waters. The phenomenon of condensation at stations S07a and S08a was clearly much less efficient resulting in less dissolution.

Accordingly, different dissolution conditions are created at different heights of a passage cross section. These differences in dissolution rate do not depend on the gypsum bedrock which is strongly isotropic, except for the presence of less soluble inclusions (e.g. well-shaped crystals or carbonate re-crystallization). Instead, there appears to be a direct relationship between dissolution and condensation rates.

Condensation rates in caves are controlled by thermal stratification inside a cave passage (Badino, 2010). The temperature gradient causing stratification depends on external heating of air particles and has seasonal effects: drier and warmer air will be present in the upper parts of the cave passages, while colder and moister air will concentrate at the bottom.

When condensation occurs (Fig. 7A), at first water moves in a laminar flow controlled by viscosity and surface tension of the water. In this condition there is only minimum dissolution. The dissolution kinetics of gypsum, in fact, is mainly controlled by the slowest process, which is the transfer of ions from the boundary layer to the solution. In a laminar water flow gypsum does not go into solution, as shown by measurements on vertical and horizontal gypsum walls in the Cava a Filo near Bologna (Forti, 2005). With the increase of the wall slope and/or the water quantity involved in the process, laminar passes to film flow, a kind of very thin water layer moving with turbulent flow, and dissolution increases reaching its highest level. This is followed by a decrease in dissolution along the cave wall because of the presence of increasing calcium and sulphate ions in solution. Finally dissolution stops due to the saturation in gypsum of the water flowing on the wall and/or to the beginning of evaporation processes. This is when gypsum deposition can start (Forti, 2004). Considering that condensation, and also evaporation, is not constant during the year but depends on several factors (e.g. temperature, relative humidity, air circulation, and so on), the sites where laminar flows transform into film flows, and the evaporation areas, change with the seasons (Fig. 7B). This defines areas in which condensation and/or evaporation can be alternatively slow and fast.

The cumulative action of these phases can explain the evolution of condensation dissolution cupolas, characterised by a flat roof and by a lower convex surface where the deposition of gypsum flowers can occur at different heights (Fig. 7B). The enlargement of the flat ceiling, by planation of the rough surface and the rock noses, is related to an increase of dissolution rate and/or flaking. Both actions lead to a mixing of boundary layers, a necessary condition for having effective dissolution. In this way, the roof enlargement is followed by the formation of a concave surface along the first few metres on the slope wall, due to increasing of the flow rate that produces higher dissolution. The progressive gypsum saturation of the flowing solution reduces the corrosion process towards the bottom of the wall. Evaporation processes can also create conditions of supersaturation; at first supersaturation

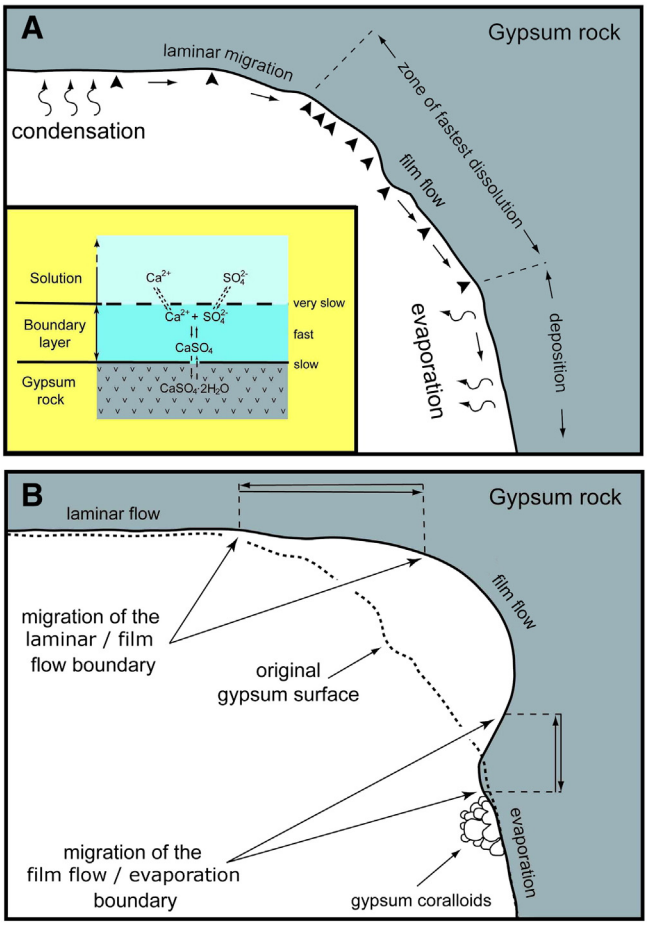

Fig. 7. Morphological evolution scheme in gypsum caves related to condensation–evaporation processes. The inset in A shows the boundary conditions of gypsum dissolution with the very slow diffusion of dissolved molecules from the boundary layer to the flowing solution. See text for explanation.

is very low and epitaxial growth favours the enlargement of existing gypsum crystals in the bedrock. Only when the supersaturation becomes important, new gypsum crystals form typical speleothems (e.g. gypsum flowers). This last phase is not frequent in the gypsum karst of Sorbas, due to the great amount of condensation water that feeds the cave system, but it can be found close to the entrances where the effectiveness of evaporation processes is amplified by the temperature increase and relative humidity decrease, as in the Covadura cave system (Fig. 8, see Fig. 1 for location). Here conductivity measurements on dripping water from stalactites fed by moist air show values around 1.8 mS/cm, testifying that gypsum speleothem precipitation leaves dripping water with a high sulphate content.

The MEM stations at the cave entrance (stations S07 and S08) only show the stage of active dissolution (film flow stage in Fig. 7) without laminar flow and gypsum speleothem precipitation.

Although the expected lowering rate on the cave floor should be less than that measured on the walls, the data from the main gallery reports the highest values of the underground measurements (an average of 0.028 and 0.022 mm yr^{-1}, for carbonate and gypsum respectively). Marginally higher mean lowering rates on gypsum sub-horizontal surfaces can be referred to stream erosion (Figs. 5–6). The differences among the various floor stations can easily be explained by fluctuations of water flow during floods and low discharge. During some periods also a very small increase has been observed in some of them. The major observed variations in downwearing and swelling are due to the characteristics of the gypsum crystals that are quickly eroded on one side and more rapidly deposited on the other: this explains the overall increase in stations S09 and S12 (Fig. 6c–d). The positive (swelling) incongruent pattern and unreasonable variations of the surface elevation on carbonate floor may be explained by calcium carbonate deposition from supersaturated water during low discharge flow but this situation requires that water should be sufficiently enriched in organic material which, by oxidation, delivers enough CO_2 to the system allowing precipitation of carbonate instead of sulphate (Dalmonte et al., 2004). This hypothesis is less probable under the current climatic conditions: in fact the gypsum area of Sorbas is semi-arid with a very low water discharge fed by condensation during most of the year, leaving flowstones dry. In addition, condensation is a process that leads to a very low CO_2 in the water, not sufficient to cause carbonate deposition. Furthermore this karst landscape is practically without vegetation, thus lacking important soil cover as a possible source of organic matter, and hindering the mechanism of the incongruent dissolution which is responsible for most of the calcite deposits in gypsum caves. A last consideration on the carbonate speleothems is that their general dryness or corrosion confirms that they must have developed during a previous speleogenetic stage. For all these reasons it is reasonable to attribute these strange values to rock surface swelling (Stephenson et al., 2004) and/or instrumental errors due to mechanical stress produced on the nails during the floods, as at the measurement point S16, in proximity to the cave stream. It is interesting to see that if these anomalous values are not considered, the mean lowering rate reaches a value of 0.020 mm yr^{-1}, very close in both kinds of substrate (gypsum and carbonate). This result should be referred to a combined chemical water dissolution during high water stands and mechanical erosion during high flows. Erosion is testified by the occurrence of clastic materials (e.g., pebbles, sands) found on the many sampling stations and by the widespread erosion morphologies like scallops, blades and potholes along the river bed. Differences between single sites can be related to the diverse location of measuring points with respect to the floods and, in particular on gypsum, also to the presence of thin clay films in between the crystals. Correlating the lowering rate and rainfall, all points on carbonate flowstones have shown an overall decrease (Fig. 6b), which indicates that the dominant process taking place on this floor is currently erosion that occurs during the flooding of the underground stream. The frequency and intensity of floods are not directly correlated to mean annual rainfall data. It should be interesting to correlate the lowering rates with each rainstorm in order to improve the knowledge on the importance of the peculiar climate of Sorbas on the cave morphology, but short-term measurements increase the errors.

Further data are available from 5 MEM stations at the surface and suggest a very fast erosion with a mean value of 0.170 mm yr^{-1}, while an even higher value (3.16 mm yr^{-1}) was obtained from the weight loss of gypsum tablets (Calaforra et al., 1993a).

In order to quantify the contribution of mechanical erosion in surface lowering, the conductivity values were used to calculate the percentage of effective rainfalls that influence the surface downwearing (about 80% of the saturation value). The quantity of removed gypsum is equal to a volume of about 70 m^3 yr^{-1} (163 t), corresponding to an average surface lowering of 0.047 mm yr^{-1}. The difference with respect to the average measured value (0.123 mm yr^{-1}) corresponds to mechanical erosion induced by the arid climate: few days of rainstorms in a generally dry climate, strong diurnal condensation which takes place practically every night and powerful winds (Shaw et al., 2011), as in Sorbas. It has to be emphasized that inside the cave most of the removed rock was surely dissolved, while at the surface the mechanical erosion is responsible for over 70% of the lowering.

Fig. 8. Morphological evidence of condensation–evaporation processes in Covadura cave system (Gypsum Karst of Sorbas) (Photo Laura Sanna).

6. Conclusions

The results of long-term MEM measurements in a gypsum cave of Sorbas (Almeria, SE Spain) have allowed quantification of the dissolution caused by condensation processes, and their possible role in speleogenesis. The data from 19 micro-erosion measurement points in four different morphological and environmental conditions show an average lowering rate of 0.014 mm yr^{-1} near the main cave entrance and of 0.016 mm yr^{-1} in the Laboratory tunnel, which can be correlated with water condensation of moist air flow triggered by thermal disequilibrium between cave and external atmospheres. Different dissolution rates are present along the cave cross-section: a slow dissolution near the ceiling, a more effective corrosion in the middle conduit wall and a very low lowering rate towards the floor. Rates of 0.022 mm yr^{-1} and 0.028 mm yr^{-1} have been recorded on gypsum bedrock and on carbonate flowstones, respectively, as cumulative effect of chemical dissolution and mechanical erosion. The denudation data from the external gypsum stations are higher, with an average of 0.170 mm yr^{-1}. In the gypsum karst of Sorbas dissolution is evaluated in an average surface lowering of 0.047 mm yr^{-1}. On the other hand, the mechanical erosion corresponds to 0.123 mm yr^{-1}. The contribution of dissolution by condensation waters to the overall karst processes in the Cueva del Agua catchment area represents over 20% of the total chemical dissolution

of the karst area and more than 50% of the speleogenetically removed gypsum in the karst system. Condensation–corrosion processes thus appear to be important in speleogenesis of gypsum caves in arid climate. At the cave scale, the morphological evidence of these processes is expressed by the evolution of dissolutional cupolas, characterised by flat roof, concave wall, and by a lower convex surface where the deposition of gypsum flowers can occur in response to sulphate supersaturation induced by evaporation. Climate factors (e.g. temperature, relative humidity, air circulation, rainfall, etc.) affect their development. Morphological evidence shows condensation–evaporation processes to be active in many cave systems of Sorbas and surely they are effective in most of the arid gypsum karsts worldwide. The same processes might also be important in both halite and limestone caves in arid climates.

Acknowledgments

The authors are grateful to Adalberto Dell'Aglio who first worked at the project in Sorbas and Carmen Guirado for her useful helping during the field work. Special thanks to Espeleo Club Almeria caving club for providing data on the Cueva del Agua. Many thanks to the two anonymous reviewers and to the editor for their comments and critical discussion of the manuscript. This research was partially funded through GLOCHARID Project grant from the Junta de Andalucía Regional Government (Spain) (code 852/2009/M/00). The author L.S. benefits from a grant supported by the European Social Funding through the Regione Autonoma della Sardegna ("Master & Back" Program — code PR-MAB-A2009-381).

References

Abu-Jaber, N., Hess, J.W., Howcroft, W., 2001. Chemical erosion of the Lilburn Cave System, Kings Canyon National Park, California. Ground Water 39, 223–229.
Audra, P., Hobléa, F., Bigot, J.-Y., Nobécourt, J.-C., 2007. The role of condensation–corrosion in thermal speleogenesis: study of a hypogenic sulfidic cave in Aix-les-Bains, France. Acta Carsol. 36, 185–194.
Auler, A.S., Smart, P.L., 2004. Rates of condensation corrosion in speleothems of semi-arid northeastern Brazil. Speleol. Evol. Karst Aquifers 2, 1–2.
Badino, G., 1995. Fisica del Clima sotterraneo. Mem. Ist. Ital. Speleol. 7, 1–137.
Badino, G., 2004. Clouds in caves. Speleol. Evol. Karst Aquifers 2, 1–8.
Badino, G., 2010. Underground meteorology — "What's the weather underground?". Acta Carsol. 39, 427–448.
Calaforra, J.M., 1986. Ideas preliminares sobra el funcionamiento hidrico del karst en yesos de Sorbas (Almeria). Lapiaz 15, 16–21.
Calaforra, J.M., 1998. Karstologìa de yesos. Universidad de Almerìa, Almeria, p. 390.
Calaforra, J.M., Pulido-Bosch, A., 1999a. Genesis and evolution of gypsum tumuli. Earth Surf. Process. Landf. 24, 919–930.
Calaforra, J.M., Pulido-Bosch, A., 1999b. Gypsum karst features as evidence of diapiric processes in the Betic Cordillera, Southern Spain. Geomorphology 29, 251–264.
Calaforra, J.M., Pulido-Bosch, A., 2003. Evolution of the gypsum karst of Sorbas (SE Spain). Geomorphology 50, 173–180.
Calaforra, J.M., Dell'Aglio, A., Forti, P., 1993a. Preliminary data on the chemical erosion in gypsum karst: 1- the Sorbas region (Spain). XIth International Congress on Speleology, Guilin, China, pp. 97–99.
Calaforra, J.M., Dell'Aglio, A., Forti, P., 1993b. The role of condensation–corrosion in the development of gypsum karst: the case of the Cueva dell'Agua (Sorbas, Spain). XIth International Congress of Speleology, Guilin, China, pp. 63–66.
Calaforra, J.M., Forti, P., Fernandez-Cortes, A., 2008. Speleothems in gypsum caves and their paleoclimatological significance. Environ. Geol. 53, 1099–1105.
Calaforra, J.M., Fernandez-Cortes, A., Gázquez Sánchez, F., Sanna, L., 2011. Proyecto GLOCHARID, Subproyecto Medio Subterraneo - Tercer informe, Septiembre 2011. Unpublished report, pp. 17.
Cigna, A.A., Forti, P., 1986. The speleogenetic role of air flow caused by convection. Int. J. Speleol. 15, 41–52.
Corbel, J., 1959. Vitesse de l'érosion. Z. Geomorphol. 3, 1–2.
Crowther, J., 1983. A comparison of the rock tablet and water hardness methods for determining chemical erosion rates on karst surfaces. Z. Geomorphol. 27, 55–64.
Cucchi, F., Forti, F., Marinetti, E., 1996. Surface degradation of carbonate rocks in the karst of Trieste (Classical Karst, Italy). In: Fornós, J.-J., Ginés, A. (Eds.), Karren Landforms, Palma de Mallorca, pp. 41–51.
Curtis, A., 2009. Karst micrometeorology of two caves on the Loser Plateau, Northern Calcareous Alps, Austria — initial results. Hoehle 60, 10–20.
Dahl, R., 1967. Postglacial microweathering of bedrock surfaces in the Narvik district of Norway. Geografiska Annaler, Series A. Phys. Geogr. 49, 23–47.
Dalmonte, C., Forti, P., Piancastelli, S., 2004. The evolution of carbonate speleothems in gypsum caves as indicators of microclimatic variations: new data from the Parco dei Gessi caves (Bologna, Italy). Mem. Ist. Ital. Speleol. 16, 65–82.
De Freitas, C.R., Schmekal, A., 2003. Condensation as a microclimate process: measurement, numerical simulation and prediction in the Glowworm Cave, New Zealand. Int. J. Climatol. 23, 557–575.
De Freitas, C.R., Schmekal, A., 2006. Studies of condensation/evaporation processes in the Glowworm Cave, New Zealand. Int. J. Speleol. 35, 75–81.
Del Monte, M., Forti, P., Tolomelli, M., 2000. Degradazione meteorica dei Gessi: nuovi dati dalle Torri Medioevali di Bologna (Italia). Atti e Memorie della Commissione "E. Boegan" 37, pp. 71–91.
Dell'Aglio, A., 1993. Misure sperimentali di erosione chimica nei gessi: il carso seccotemperato di Sorbas (Almeria, Spagna)(MSc. Thesis) Dipartimento di Scienze della Terra e Geologico-Ambientali, University of Bologna, Bologna, p. 90.
Dreybrodt, W., Gabrovšek, F., Perne, M., 2005. Condensation corrosion: a theoretical approach. Acta Carsol. 34, 317–348.
Dronkert, H., 1977. The evaporites of the Sorbas Basin. Rev. Inst. Inv. Geol. Diput. Barcelona 33, 55–76.
Dublyansky, V.N., Dublyansky, Y.V., 2000. The role of condensation in karst hydrogeology and speleogenesis. In: Klimchouk, A., Ford, D.C., Palmer, A.N., Dreybrodt, W. (Eds.), Speleogenesis: Evolution of Karst Aquifers. National Speleological Society, Huntsville, pp. 100–112.
Ford, D.C., 1971. Research methods in karst geomorphology. Proc. Guelph Symp. Geomorph., Guelph, pp. 23–47.
Forti, P., 2004. Gypsum karst. In: Goudie, A.S. (Ed.), Encyclopedia of Geomorphology, New York, pp. 509–511.
Forti, P., 2005. Degradazione meteorica dei gessi: nuovi dati dalla Cava Filo (Parco dei Gessi Bolognesi). Speleol. Emiliana 14–15, 15–19.
Furlani, S., Cucchi, F., Forti, F., Rossi, A., 2009. Comparison between coastal and inland Karst limestone lowering rates in the northeastern Adriatic Region (Italy and Croatia). Geomorphology 104, 73–81.
Furlani, S., Cucchi, F., Odorico, R., 2010. A new method to study microtopographical changes in the intertidal zone: one year of TMEM measurements on a limestone removable rock slab (RRS). Z. Geomorphol. N.F. 54, 137–151.
Gabrovšek, F., 2009. On concepts and methods for the estimation of dissolutional denudation rates in karst areas. Geomorphology 106, 9–14.
Gabrovšek, F., Dreybrodt, W., Perne, M., 2010. Physics of condensation corrosion in caves. In: Andreo, B., Carrasco, F., Durán, J.J., LaMoreaux, J.W. (Eds.), Advances in Research in Karst Media, Heidelberg, pp. 491–496.
Gams, I., 1986. International comparative measurements of surface solution by means of standard limestone tablets. Zb. Ivana Rakovca 26, 361–386.
Groves, C., Meiman, J., 2005. Weathering, geomorphic work, and karst landscape evolution in the Cave City groundwater basin, Mammoth Cave, Kentucky. Geomorphology 67, 115–126.
Gunn, J., 1981. Limestone solution rates and processes in the Waitomo district, New-Zealand. Earth Surf. Process. Landf. 6, 427–445.
Gutierrez, F., Calaforra, J.M., Cardona, F., Orti, F., Duran, J.J., Garay, P., 2008. Geological and environmental implications of the evaporite karst in Spain. Environ. Geol. 53, 951–965.
Hanna, F.K., 1966. A technique for measuring the rate of erosion of cave passages. Proc. Univ. Bristol Spelaeol. Soc. 11, 83–86.
Häuselmann, P., 2008. Surface corrosion of an Alpine karren field: recent measures at Innerbergli (Siebenhengste, Switzerland). Int. J. Speleol. 37, 107–111.
High, C.J., Hanna, F.K., 1970. Method for the direct measurements of erosion on rock surfaces. Br. Geomorphol. Res. Group Tech. Bull. 5, 1–25.
Jones, P., Harris, I., 2011. Climate data provided by CRU TS 3.1 — University of East Anglia Climate Research Unit (CRU). CRU Time Series (TS) high resolution gridded datasets([Internet]) NCAS British Atmospheric Data Centre, 2008. (Accessed: 28-July-2010).
Klimchouk, A.B., 2000. Dissolution and conversions of gypsum and anhydrite. In: Klimchouk, A., Ford, D.C., Palmer, A.N., Dreybrodt, D. (Eds.), Speleogenesis. Evolution of Karst Aquifers. National Speleological Society, Huntsville, pp. 160–168.
Klimchouk, A.B., Aksem, S.D., 2002. Gypsum karst in the western Ukraine: hydrochemistry and solution rates. Carbonates Evaporites 17, 142–153.
Klimchouk, A.B., Aksem, S.D., 2005. Hydrochemistry and solution rates in gypsum karst: case study from the Western Ukraine. Environ. Geol. 48 (3), 307–319.
Klimchouk, A.B., Cucchi, F., Calaforra, J.M., Aksem, S., Finocchiaro, F., Forti, P., 1996a. Dissolution of gypsum from field observations. Int. J. Speleol. 25 (3–4), 37–48.
Klimchouk, A.B., Lowe, D.J., Cooper, A.H., Sauro, U. (Eds.), 1996b. Gypsum karst of the world. International Journal of Speleology 25 (3–4), p. 308.
Lauritzen, S.E., 1990. Autogenic and allogenic denudation in carbonate karst by the Multiple Basin Method — an example from Svartisen, North Norway. Earth Surf. Process. Landf. 15, 157–167.
Maestre, F.T., Escolar, C., Ladron de Guevara, M., Quero, J.L., Lazaro, R., Delgado-Baquerizo, M., Ochoa, V., Berdugo, M., Gozalo, B., Gallardo, A., 2013. Changes in biocrust cover drive carbon cycle responses to climate change in drylands. Glob. Chang. Biol. 19, 3835–3847.
Mather, A.E., Harvey, A.M., 1995. Controls on drainage evolution in the Sorbas Basin, SE Spain. In: Lewin, J., Macklin, M.G., Woodward, J.C. (Eds.), Mediterranean Quaternary River Environments, Balkema, Rotterdam, pp. 65–76.
Plan, L., 2005. Factors controlling carbonate dissolution rates quantified in a field test in the Austrian alps. Geomorphology 68, 201–212.
Plan, L., Tschegg, C., De Waele, J., Spötl, C., 2012. Corrosion morphology and cave wall alteration in an Alpine sulfuric acid cave (Kraushöhle, Austria). Geomorphology 169–170, 45–54.
Pulido Bosch, A., 1986. Le karst dans les gyses de Sorbas (Almeria). Aspects morphologiques et hydrogéologiques. Karstol. Mem. 1, 27–35.
Pulido Bosch, A., 2007. Nociones de hidrogeologia para ambientologos. Universidad de Almeria, Almeria pp 492.
Pulido Bosch, A., Calaforra, J.M., 1993. The gypsum karstic aquifer of Sorbas (Almería). In: Pulido Bosch, A. (Ed.), Some Spanish Karstic Aquifers, Granada, pp. 225–241.

Pulina, M., Sauro, U., 1993. Modello dell' erosione chimica potenziale di rocce carbonatiche in Italia. Mem. Soc. Geol. Ital. 49, 313–323.
Roep, T.B., Beets, D.J., Dronkert, H., Pagnier, H., 1979. A prograding coastal sequence of wave-built structures of Messinian age, Sorbas, Almeria, Spain. Sediment. Geol. 22, 135–163.
Roveri, M., Gennari, R., Lugli, S., Manzi, V., 2009. The terminal carbonate complex: the record of sea-level changes during Messinian salinity crisis. GeoActa 8, 63–70.
Ruegg, G.H., 1964. Geologische onderzoekingen in het bekken van Sorbas, SE Spanje, Geologisch Instituut. Universiteit van Amsterdam, Amsterdam, p. 67.
Sanna, L., Gazquez, F., Calaforra, J.M., 2012. A geomorphological and speleological approach in the study of hydrogeology of gypsum karst of Sorbas (SE Spain). Geogr. Fis. Din. Quat. 35, 153–166.
Shaw, M.G., Stafford, K.W., Tate, B.P., 2011. Surface denudation of the Gypsum Plain, West Texas and Southeastern New Mexico. In: Kuniansky, E.L. (Ed.), U.S. Geological Survey Karst Interest Group Proceedings, Fayetteville, Arkansas, April 26–29, 2011, U.S. Geological Survey Scientific Investigations Report 2011-5031, pp. 104–112.
Smith, D.I., 1978. The micro erosion meter: its application to the weathering of rock surfaces. In: Pearson, C. (Ed.), Conservation of Rock Art, Sydney, pp. 44–53.
Spate, A.P., Jennings, J.N., Smith, D.I., Greenaway, M.A., 1985. The micro-erosion meter — use and limitations. Earth Surf. Process. Landf. 10, 427–440.
Stephenson, W.J., 1997. Improving the traversing micro-erosion meter. J. Coast. Res. 13, 236–241.
Stephenson, W.J., Finlayson, B.L., 2009. Measuring erosion with the micro-erosion meter–contributions to understanding landform evolution. Earth Sci. Rev. 95, 53–62.
Stephenson, W.J., Taylor, A.J., Hemmingsen, M.A., Tsujimoto, H., Kirk, R.M., 2004. Short-term microscale topographic changes of coastal bedrock on shore platforms. Earth Surf. Process. Landf. 29, 1663–1673.
Stephenson, W.J., Kirk, R.M., Hemmingsen, S.A., Hemmingsen, M.A., 2010. Decadal scale micro erosion rates on shore platforms. Geomorphology 114, 22–29.
Tarhule-Lips, R.F.A., Ford, D.C., 1998. Condensation corrosion in caves on Cayman Brac and Isla de Mona. J. Cave Karst Stud. 60, 84–95.
Trenhaile, A.S., Lakhan, V.C., 2011. Transverse micro-erosion meter measurements; determining minimum sample size. Geomorphology 134, 431–439.
Trudgill, S., 1970. Micro-erosion measurement of exposed bedrock. Area 3, 61.
Trudgill, S., 1975. Measurements of erosional weight loss of rock tablets. Br. Geomorphol. Res. Group Tech. Bull. 17, 13–19.
Trudgill, S., High, C.J., Hanna, K.K., 1981. Improvements to the micro-erosion meter (MEM). Br. Geomorphol. Res. Group Tech. Bull. 29, 3–17.